JOINT DETECTION AND DECODING OF LDPC CODED DISTRIBUTED SPACE-TIME SIGNALING IN WIRELESS RELAY NETWORKS VIA LINEAR PROGRAMMING

Kun Wang, Wenhao Wu and Zhi Ding

Department of Electrical and Computer Engineering
University of California, Davis, CA 95616
{kunwang,wnhwu,zding}@ucdavis.edu

ABSTRACT

We develop a linear programming based approach for the joint detection and decoding of LDPC coded distributed space-time signaling transmitted in a wireless relay network. Traditional receivers typically decouple the detection and decoding processes as two separate blocks or require iterative turbo exchange of extrinsic information between the soft detector and decoder. We exploit the constraints imposed on the channel input signals and jointly consider the training symbols as well as the LDPC code information by formulating a unified linear programming (LP) receiver. Moreover, in consideration of the vast amount of LDPC parity check inequalities, we present an adaptive procedure to significantly reduce the complexity of the proposed LP receiver.

Index Terms— Linear programming, LDPC, joint detection and decoding, space-time signaling.

1. INTRODUCTION

This work focuses on joint detection and decoding of LDPC coded wireless transmissions over multiple-input multiple-output (MIMO) systems. For MIMO transmission, space-time code (STC) has proven highly effective in its ability to deliver high throughput and full spatial diversity gain without prior channel information. While space-time MIMO transmission requires multiple co-located transmit antennas, distributed space-time code (DSTC) transmission becomes a natural alternative for smaller mobile devices with size constraint by letting multiple single antenna nodes to form virtual MIMO systems [1]. The detection of STC signals has been investigated in the literature [2, 3], typically relying on estimated channel information at the receiver. When STC or DSTC transmitters fail to provide sufficient pilot symbols for channel estimation, however, blind detection of STC including the full rate Alamouti code has also been proposed in [4] to achieve near-maximum-likelihood performance.

In spite of the much improved capacity, wireless channel fading and noise effects can still lead to substantial detection errors. In practice, forward error correction (FEC) codes are routinely adopted in conjunction with MIMO systems. For over a decade, LDPC codes have become highly popular owing to their excellent error correction performance [5, 6]. LDPC codes, when decoded via the simple sum-product algorithm (SPA), can approach Shannon limit with reasonable decoding complexity [7]. When LDPC codes are applied in MIMO-OFDM transmissions [8], the receiver should ideally apply a joint maximum likelihood (ML) detection and decoding algorithm. However, if the LDPC codes are sufficiently long, such an optimum joint receiver is too complex and difficult to implement.

Most STC detection algorithms for MIMO system are separate from the FEC code decoder. The reason lies in the fact that symbol detection in STC typically operates in either the real or the complex field while FEC decoding generally operates in the Galois field. Despite the success of sum-product algorithm (SPA) for LDPC decoding, its high nonlinearity during message passing makes it challenging to integrate with the MIMO detection step. Thus, joint MIMO detection and FEC decoding receivers in the literature are typically based on the exchange of soft information to form a turbo-equalizer/detector [9, 10]. Nevertheless, these belief propagation based turbo receivers do not admit a unified optimization formulation. The convergence of such iterative receivers is also less predictable while exchanging unreliable soft information at low to moderate SNRs may even worsen both detection and decoding.

Recently, Feldman *et al.* [11] proposed an LP-based LDPC decoding scheme, which is amendable to existing detection algorithms. By taking the advantage of LP decoding, Cui *et al.* [12] proposed an l_1 norm based joint detector and decoder for MIMO systems, but it cannot directly tackle higher-order modulations. In [13], Flanagan developed a unified framework for LP receivers, and more recently Li *et al.* [14] generalized Flanagan's method to MIMO-OFDM systems. We note that all these methods assume perfect channel state information (CSI) or closed-form estimates at the receiver.

In this work, we present a new joint detection and decoding algorithm for LDPC-coded DSTC transmissions. Utilizing the *minimum peak distortion* (MPD) criterion that targets QAM data symbols, we exploit limited pilot symbols to avoid the all-zero trivial solution and to resolve rotational ambiguities. We further improve the joint receiver performance by incorporating the LDPC code information through a set of LP decoding constraints. We also apply a subspace approach for noise suppression. Since both QAM data symbols and lim-

This material is based on works supported by the National Science Foundation Grants CNS-1147930, ECCS-1307820 and CIF-1321143.

978-1-4799-2893-4/14/$31.00 ©2014 IEEE

ited pilot symbols take part in receiver optimization, this joint detection-decoding receiver is semi-blind in nature. The unification of MIMO detection, pilot symbol, LDPC code and subspace separation constraints in this LP receiver can help improve the detection performance and data reliability.

We note that the MPD criterion using LP was first proposed for blind equalization of single antenna data transmission in [15], and was later extended in [16] to include pilot constraints and LDPC code constraints for single-input single-output (SISO) inter-symbol interference (ISI) channel. Our new work in this paper represents a non-trivial extension to LDPC coded DSTC systems. We also substantially reduced the receiver complexity without sacrificing performance in order to accommodate practical (longer) LDPC codes.

2. DISTRIBUTED SPACE-TIME TRANSMISSION

Consider the block diagram of a distributed wireless relay network shown in Fig. 1 with one transmitter, one receiver, and multiple amplify-forward (AF) relays. The transmitter, receiver and relays are assumed to possess 1 transmit antenna, N receive antennas, and a total of R relay antennas, respectively. Independent Rayleigh flat-fading channels are assumed for both transmitter-relay and relay-receiver channels. Furthermore, a quasi-static fading channel lasting for two hops is assumed. We let the data symbols $\{s_l\}_{l=1}^{n_s}$ be generated from a square QAM constellation $\mathcal{A}$ that satisfies $M = \max_{s_l\in\mathcal{A}} |\mathrm{Re}\{s_l\}| = \max_{s_l\in\mathcal{A}} |\mathrm{Im}\{s_l\}|$.

We now describe the half-duplex two-phase relay protocol for the DSTC network [17]. Without loss of generality, consider one block of n_s symbols. During the first phase, the symbols $\mathbf{s} = [s_1\ \ldots\ s_{n_s}]^T$, normalized as $\mathbb{E}\{\mathbf{s}^H\mathbf{s}\} = n_s$, are transmitted. The i-th relay antenna receives signal

$$\mathbf{r}_i = \sqrt{P_s} f_i \mathbf{s} + \mathbf{n}_{r,i}, \quad 1 \le i \le R \tag{1}$$

where P_s is the average transmit power, $f_i \sim \mathcal{CN}(0, \sigma_f^2)$ is the channel gain from the transmitter antenna to the i-th relay antenna, and $\mathbf{n}_{r,i}$ is the complex additive white Gaussian noise (AWGN).

Upon receiving $\mathbf{r}_i$, the i-th AF relay linearly processes $\mathbf{r}_i$ and its conjugate $\mathbf{r}_i^*$ by using the $L \times n_s$ precoding matrices $\mathbf{A}_i$ and $\mathbf{B}_i$, respectively.

$$\mathbf{t}_i = \sqrt{\frac{P_r}{P_s+1}}(\mathbf{A}_i\mathbf{r}_i + \mathbf{B}_i\mathbf{r}_i^*) = \sqrt{\frac{P_r}{P_s+1}}\breve{\mathbf{A}}_i\breve{\mathbf{r}}_i \tag{2}$$

where P_r is the average transmit power for each relay antenna. Note that, for simplicity, we only consider two special cases that either $\mathbf{A}_i = \mathbf{0}, \mathbf{B}_i$ is unitary or $\mathbf{A}_i$ is unitary, $\mathbf{B}_i = \mathbf{0}$ in Eq. (2). In other words, $\breve{\mathbf{A}}_i$ is either $\mathbf{A}_i$ or $\mathbf{B}_i$, and $\breve{\mathbf{r}}_i$ is either $\mathbf{r}_i$ or $\mathbf{r}_i^*$ [18].

In the second phase, the relay nodes send signals to the receiver. Assuming signals from all relays share the same channel and are synchronized, the received signal matrix $\mathbf{Y}$ at the receiver is simply

$$\mathbf{Y} = \mathbf{G}\left[\mathbf{t}_1\ \ldots\ \mathbf{t}_R\right]^T + \mathbf{N}_d \tag{3}$$

where $\mathbf{G}$ is an $N \times R$ channel matrix with each element following $\mathcal{CN}(0, \sigma_G^2)$ and $\mathbf{N}_d$ is an AWGN matrix.

By defining $\beta \triangleq P_s P_r (P_s + 1)^{-1}$, we can write the transceiver equation in a more compact form

$$\mathbf{Y} = \sqrt{\beta}\tilde{\mathbf{\Psi}}\mathbf{S} + \mathbf{W} \tag{4}$$

where
$$\mathbf{S} \triangleq \left[\breve{\mathbf{A}}_1\breve{\mathbf{s}}\ \ldots\ \breve{\mathbf{A}}_R\breve{\mathbf{s}}\right]^T, \tag{5}$$

$$\tilde{\mathbf{\Psi}} \triangleq \mathbf{G}\,\mathrm{diag}\{\breve{f}_1, \ldots, \breve{f}_R\}, \tag{6}$$

$$\mathbf{W} \triangleq \sqrt{\frac{P_r}{P_s+1}}\mathbf{G}\left[\breve{\mathbf{A}}_1\breve{\mathbf{n}}_{r,1}\ \ldots\ \breve{\mathbf{A}}_R\breve{\mathbf{n}}_{r,R}\right]^T + \mathbf{N}_d. \tag{7}$$

Analogous to multiple-antenna STC, $\tilde{\mathbf{\Psi}}$ is the end-to-end channel matrix, $\mathbf{S}$ is the distributed space-time codeword whereas $\mathbf{W}$ is the equivalent (colored) noise at the receiver.

To simplify later derivations, the standard DSTC is transformed to an *equivalent spatial diversity* (ESD) model that converts the space-time structure into the channel [4].

$$\mathbf{y} = \sqrt{\beta}\mathbf{\Psi}\mathbf{s} + \mathbf{w}. \tag{8}$$

For the case of the rate 1 Alamouti code

$$\tilde{\mathbf{\Psi}} = \begin{bmatrix}\tilde{\boldsymbol{\psi}}_1 & \tilde{\boldsymbol{\psi}}_2\end{bmatrix} \Rightarrow \mathbf{\Psi} = \begin{bmatrix}\tilde{\boldsymbol{\psi}}_1 & \tilde{\boldsymbol{\psi}}_2 \\ \tilde{\boldsymbol{\psi}}_2^* & -\tilde{\boldsymbol{\psi}}_1^*\end{bmatrix} \tag{9}$$

$$\mathbf{y} = \begin{bmatrix}\mathbf{Y}(:,1) \\ \mathbf{Y}(:,2)^*\end{bmatrix}, \mathbf{w} = \begin{bmatrix}\mathbf{W}(:,1) \\ \mathbf{W}(:,2)^*\end{bmatrix} \tag{10}$$

in which the Matlab notation $\mathbf{D}(:,i)$ is used to represent the i-th column of matrix $\mathbf{D}$.

3. JOINT DSTC DETECTION AND DECODING

To start our receiver design, we consider K blocks of data symbols. Moreover, both sides of Eq. (8) are divided by $\sqrt{\beta}$. With a little abuse of notations on the noise vector, the new ESD transceiver equation is

$$\mathbf{y}[k] = \mathbf{\Psi}\mathbf{s}[k] + \mathbf{w}[k], \quad 1 \le k \le K. \tag{11}$$

Here we define the optimization criterion based on QAM symbols before various constraints to tighten the solution.

3.1. Convex Peak Distortion Cost Function

Let $\mathbf{\Theta} = [\boldsymbol{\theta}_1\ \ldots\ \boldsymbol{\theta}_{n_s}] \in \mathcal{C}^{NL\times n_s}$ denote linear detector (matrix) for the ESD model. Therefore, the detection output $\hat{\mathbf{s}}[k] = \mathbf{\Theta}^H\mathbf{y}[k]$. It is thus clear that the l-th column $\boldsymbol{\theta}_l$ of the matrix $\mathbf{\Theta}$ is for recovering the l-th symbol $\hat{s}_l[k] = \boldsymbol{\theta}_l^H\mathbf{y}[k]$ in equalized data vector $\hat{\mathbf{s}}[k]$.

Given QAM signal transmission, we apply the MPD criterion proposed in [15]. Specifically, define the cost function for the l-th equalizer $\boldsymbol{\theta}_l$ as

$$\begin{aligned}\mathbf{J}(\boldsymbol{\theta}_l) =& \frac{1}{2M}\max_k[|\mathrm{Re}\{\hat{s}_l[k]\}| + |\mathrm{Im}\{\hat{s}_l[k]\}|] \\ =& \sum_{j=1}^{n_s}[|\mathrm{Re}\{c_{j,l}\}| + |\mathrm{Im}\{c_{j,l}\}|]\end{aligned} \tag{12}$$

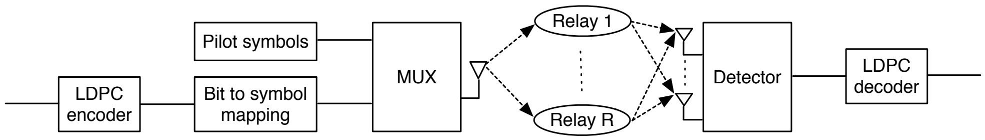

Fig. 1. System Model for DSTC

where $\mathbf{c}_l^T = \boldsymbol{\theta}_l^H \boldsymbol{\Psi} = [c_{1,l} \ldots c_{n_s,l}]$ is the l-th concatenated channel-detector response vector. Because the objective function $\mathbf{J}(\boldsymbol{\theta}_l)$ is convex in $|\mathrm{Re}\{c_{j,l}\}|$ and $|\mathrm{Im}\{c_{j,l}\}|$ while the concatenated response $\mathbf{c}_l$ is linear in $\boldsymbol{\theta}_l$, we can see that $\mathbf{J}(\boldsymbol{\theta}_l)$ is a convex function of $\boldsymbol{\theta}_l$. Note that the minimization of $\mathbf{J}(\boldsymbol{\theta}_l)$ without constraint would result in a trivial solution $\boldsymbol{\theta}_l = \mathbf{0}$. It is therefore important to define proper constraints to avoid the all-zero output solution.

3.2. Pilot Constraints Integration

To prevent the minimization of $\mathbf{J}(\boldsymbol{\theta}_l)$ from becoming trivial, a simple *anchor tap constraint* is adopted in [4] and [15] for blind equalization. Such constraint, however, is insensitive to phase-rotational and scalar-multiplicative ambiguities. As a result, further integration with other constraints can be challenging. To resolve the triviality and ambiguities, we propose to apply a limited number of pilot constraints.

Ideally, we expect the detector output to match the pilot. However, in the presence of channel noise, the exact pilot constraint $\hat{s}_l[k] = p_l[k]$ typically does not hold. Instead, we propose to apply constraints in the form of *squeezing box* [16].

$$|\mathrm{Re}\{\hat{s}_l[k]\} - \mathrm{Re}\{p_l[k]\}| \le \tau_p^R[k], \qquad k \in K_P \tag{13a}$$

$$|\mathrm{Im}\{\hat{s}_l[k]\} - \mathrm{Im}\{p_l[k]\}| \le \tau_p^I[k], \qquad k \in K_P \tag{13b}$$

where K_P is the pilot index set; $\tau_p^R[k]$'s and $\tau_p^I[k]$'s are optimization variables to be included in the objective function.

3.3. LDPC Codeword Constraints

We advocate the integration of detection and decoding at the receiver in a unified optimization process. Instead of applying the transitional belief propagation between the MAP detector and the SPA decoder in turbo equalization, we would like to incorporate a set of convex (and in fact, linear) constraints generated from the LDPC binary constraints.

Consider an LDPC parity check matrix $\mathbf{H}$ with M_c rows and N_c columns. Denote the set of neighbors of the m-th check node as $\mathcal{N}_m$. For a subset $\mathcal{F} \subseteq \mathcal{N}_m$ with odd cardinality $|\mathcal{F}|$, we can get the following polytope constraints [11]

$$\sum_{n \in \mathcal{F}} f[n] - \sum_{n \in (\mathcal{N}_m \backslash \mathcal{F})} f[n] \le |\mathcal{F}| - 1 \tag{14a}$$

$$0 \le f[n] \le 1 \tag{14b}$$

where $f[n]$ is the n-th bit in an LDPC codeword.

To incorporate the polytope constraints that involve the information bits, we need to employ additional constraints that connect information bits $\{f[n]\}$ and the QAM symbols $\{z[k]\}$. Taking 4-QAM as an example, the Gray mapping between symbols and bits admits the affine relationship

$$z[k] = ((1 - 2f[2k]) + j(1 - 2f[2k-1]))\,/\sqrt{2} \tag{15}$$

where the complex QAM symbol $z[k] \in \mathcal{A}$. Under noise, the detector output sample does not exactly match the QAM constellation point. For this reason, we again use the *squeezing box* technique to relax the LDPC constraints as

$$|\mathrm{Re}\{\hat{s}_l[k]\} - \mathrm{Re}\{z[k]\}| \le \tau_c^R[k], \qquad k \in K_D \tag{16a}$$

$$|\mathrm{Im}\{\hat{s}_l[k]\} - \mathrm{Im}\{z[k]\}| \le \tau_c^I[k], \qquad k \in K_D \tag{16b}$$

where K_D is the data symbol index set.

3.4. Subspace Separation Constraints

Another condition we exploit is the orthogonality between signal and noise subspace. A clean signal $\mathbf{y}_s[k] = \boldsymbol{\Psi}\mathbf{s}[k]$ lies in the column space of $\boldsymbol{\Psi}$. The noisy signal $\mathbf{y}[k]$ can be decomposed into column space of $\boldsymbol{\Psi}$ and the null space of $\boldsymbol{\Psi}^T$, denoted as $\mathcal{R}(\boldsymbol{\Psi})$ and $\mathcal{R}(\boldsymbol{\Psi}^\perp)$, respectively. We want the detector $\boldsymbol{\theta}_l$ to be orthogonal to $\mathcal{R}(\boldsymbol{\Psi}^\perp)$ so as not to waste effort in subspace without any signal component.

Singular value decomposition (SVD) on a frame of data

$$[\mathbf{y}[1] \ldots \mathbf{y}[K]] = \mathbf{U}\boldsymbol{\Lambda}\mathbf{V}^H = [\,\underbrace{\mathbf{U}_s}_{n_s} \; \underbrace{\mathbf{U}_n}_{NL-n_s}\,]\boldsymbol{\Lambda}\mathbf{V}^H \tag{17}$$

where $\mathbf{U}$ and $\mathbf{V}$ are unitary. $\mathbf{U}_n$ spans the noise space, i.e., $\mathcal{R}(\boldsymbol{\Psi}^\perp) = \mathcal{R}(\mathbf{U}_n)$. Therefore, we have the following subspace separation constraints

$$\mathbf{U}_n^H \boldsymbol{\theta}_l = 0. \tag{18}$$

4. UNIFIED LP AND COMPLEXITY REDUCTION

To summarize, our unified LP (**ULP**) for the detection of DSTC is as follows:

$$\begin{aligned}
\min_{\boldsymbol{\theta}_l}.\quad & \lambda_{eq}(\tau_{eq}^R + \tau_{eq}^I) + \lambda_p \sum_{k=1}^{|K_P|} (\tau_p^R[k] + \tau_p^I[k]) \\
& + \lambda_c \sum_{k=1}^{|K_D|} (\tau_c^R[k] + \tau_c^I[k]) \\
\text{s.t.}\quad & -\tau_{eq}^R \le \mathrm{Re}\{\hat{s}_l[k]\} \le \tau_{eq}^R,\ k \in K_D \\
& -\tau_{eq}^I \le \mathrm{Im}\{\hat{s}_l[k]\} \le \tau_{eq}^I,\ k \in K_D \\
& [\text{Pilot Constraints (13)}] \\
& [\text{LDPC Constraints (14) (15) (16)}] \\
& [\text{Subspace Constraints (18)}] \\
& \tau_{eq}^R, \tau_{eq}^I, \tau_p^R[k], \tau_p^I[k], \tau_c^R[k], \tau_c^I[k] \ge 0
\end{aligned} \tag{19}$$

where λ_{eq}, λ_p and λ_c are weights applied for MPD cost, pilot constraints, and LDPC code constraints, respectively. Note that after recovering $\boldsymbol{\theta}_l$, we can utilize the code-dependent mapping to obtain the remaining columns of $\boldsymbol{\Theta}$; cf. [4].

We note that the ULP in (19) has a complexity issue. In fact, the total number of constraints and consequently the complexity of the unified LP would be quite high for long LDPC codes or codes of large row weights. For complexity reduction at the receiver, we can adopt the cutting plane method [20] in which only violated parity check inequalities are added. Accordingly, our adaptive LP (**ALP**) receiver works as follows:

- S1 Initialize the LP detection without constraints (14a).
- S2 Solve the current LP to obtain the detector $\boldsymbol{\theta}_l$ and demodulate the symbols to bits $\{f[n], 1 \leq n \leq N_c\}$.
- S3 If cuts (violated constraints) are found by using $\{f[n]\}$, add them to LP and return to S2; otherwise, go to S4.
- S4 Use mapping to obtain $\boldsymbol{\Theta}$ and detect frame symbols.

5. SIMULATIONS

To empirically illustrate performance of the proposed receivers, we test rate-1/2 LDPC codes of different lengths, listed in Table 1 [21]. For comparison, we test the LP receiver without LDPC constraints (14) (15) (16) and label this receiver as disjoint LP (**DLP**). We also compare our results against pure training-based ML detection that uses least square channel estimate.

In the simulations, we choose 4-QAM data transmission. The network has 1 transmit antenna, 2 relay nodes each with 1 antenna, and 2 receive antennas. The source-relay and relay-destination channel coefficients and noise elements all follow $\mathcal{CN}(0, 1)$. We apply the optimum power allocation $P_s = RP_r$ [17]. Our DSTC uses Alamouti code. Two pilot symbols are transmitted from the source; one is chosen from the QAM constellation and the other is 0. As for the choice of weights λ's in the cost function, we set $\lambda_p = 100$, whereas $\lambda_{eq} = 1$ and $\lambda_c = 1$. Moreover, we whiten the noise at the detector output before applying SPA to further improve BER.

First, consider an LDPC code of length 204. Fig. 2 shows that ALP maintains the same BER performance as ULP. Moreover, we test an LDPC code of practical length, as shown in Fig. 3. To be fair, we examine all results of different methods after SPA. The proposed ULP outperforms DLP and traditional ML receivers by 1dB and 2dB, respectively.

Next, we study the complexity reduction by ALP. We use the commercial LP solver, MOSEK [22], to numerically evaluate the complexity in terms of the Floating-Point Operations (FLOPS) that LP receiver algorithm uses. Consider $P_s = 20$ dB. Table 1 illustrates a substantial complexity reduction as ALP can be several orders of magnitude faster than ULP.

6. CONCLUSIONS

This work presents a new unified detection-decoding receiver formulation for DSTC relay networks. Unlike traditional disjoint or belief propagation receivers, we jointly utilize the feature of QAM signals, the available pilots, and LDPC code constraints in an integrated linear programming receiver algorithm. Our receiver manifests as a single constrained optimization formulation. We also reduce the algorithm complexity to make it work for practically long LDPC codes. The proposed LP shows good performance in our simulation tests. Future works will address the generalization to higher-order QAM and integration of other a priori signaling information.

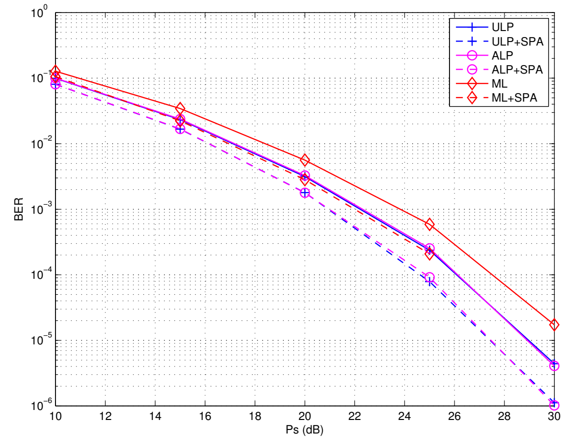

Fig. 2. BER comparison of (204,102) LDPC code.

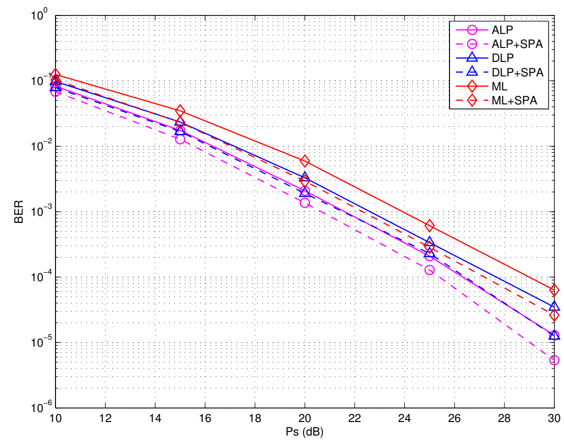

Fig. 3. BER comparison of (1008,504) LDPC code.

Table 1. FLOPS comparison of ULP and ALP

Code Length	FLOPS of ULP	FLOPS of ALP
204	1.33×10^6	1.51×10^5
504	9.50×10^6	3.71×10^5
1008	7.30×10^7	7.41×10^5
2640	8.28×10^8	1.94×10^6

7. REFERENCES

[1] Y. Jing and B. Hassibi, "Distributed space-time coding in wireless relay networks," *IEEE Trans. Wireless Commnu.*, vol. 5, no. 12, pp. 3524-3536, Dec. 2006.

[2] P. Stoica and G. Ganesan, "Space-time block codes: Trained, blind and semi-blind detection," in *Proc. IEEE ICASSP 2002*, Orlando, USA, Oct. 2002.

[3] Z. Ding and D. B. Ward, "Subspace approach to blind and semi-blinding channel estimation for space-time block codes," *IEEE Trans. Wireless Commun.*, vol. 4, no. 2, pp. 357-362, Mar. 2005.

[4] M. Zia and Z. Ding, "A linear programming receiver for blind detection of full rate space-time block codes," *IEEE Trans. Signal Process.*, vol. 58, no.11, pp. 5819-5834, Nov. 2010.

[5] R. G. Gallager, "Low-density parity-check codes," *IRE Trans. Inf. Theory*, vol. 8, pp. 21-28, Jan. 1962.

[6] D. J. C. MacKay and R. M. Neal, "Good error-correcting codes based on very sparse matrices," *IEEE Trans. Inf. Theory*, vol. 45, no. 2, pp. 399-431, Mar. 1999.

[7] T. J. Richardson and R. Urbanke, "The capacity of low-density parity-check codes under message-passing decoding," *IEEE Trans. Inf. Theory*, vol. 47, pp. 599-618, Feb. 2001.

[8] H.-N. Lee, "LDPC coded modulation MIMO OFDM transceiver: Performance comparison with MAP equalization," in *Proc. 2003 VTC - Spring*, vol. 2, pp. 1178-1182.

[9] B. Lu, G. Yue, and X. Wang, "Performance analysis and design optimization of LDPC coded MIMO OFDM systems," *IEEE Trans. Signal Process.*, vol. 52, no. 2, pp. 348-361, Nov. 2004.

[10] M. C. Reed, C. B. Schlegel, P. D. Alexander, and J. A. Asenstorfer, "Iterative multiuser detection for CDMA with FEC: near-single-user performance," *IEEE Trans. Commun.*, vol. 46, no. 12, pp. 1693-1699, Dec. 1998.

[11] J. Feldman and D. Karger, "Using linear programming to decode binary linear codes," *IEEE Trans. Inf. Theory*, vol. 51, no. 3, pp. 954-972, Mar. 2005.

[12] T. Cui, T. Ho, and C. Tellambura, "Linear programming detection and decoding for MIMO systems," in *Proc. IEEE ISIT 2006*, Seattle, USA, July 2006.

[13] M. F. Flanagan, "A unified framework for linear-programming based communication receiver," *IEEE Trans. Inf. Theory*, vol. 59, no. 12, pp. 3375-3387, Apr. 2011.

[14] Y. Li, L. Wang, and Z. Ding, "Linear programming based joint detection of LDPC coded MIMO systems," in *Proc. IEEE Globecom 2012*, Anaheim, USA, Dec. 2012.

[15] Z. Ding and Z.-Q. Luo, "A fast linear programming algorithm for blind equalization," *IEEE Trans. Commun.*, vol. 48, no. 9, pp. 1432-1436, Sept. 2000.

[16] N. Jacklin and Z. Ding, "On efficient utilization of training pilots for linear equalization of QAM transmissions," *IEEE Trans. Commun.*, vol. 61, no. 12, pp. 4984-4996, Dec. 2013..

[17] Y. Jing, *Distributed Space-time Coding*, Springer, 2013.

[18] Y. Jing and H. Jafarkhani, "Using orthogonal and quasi-orthogonal designs in wireless relay networks," *IEEE Trans. Inf. Theory*, vol. 53, no. 11, pp. 4106-4118, Nov. 2007.

[19] A.-J. Van Der Veen, E. F. Deprettere, and A. L. Swindlehurst, "Subspace based signal analysis using singular value decomposition," *Proc. IEEE*, vol. 81, no. 9, pp. 1277-1308, Sept. 1993.

[20] M. H. Taghavi N. and P. H. Siegel, "Adaptive methods for linear programming decoding," *IEEE Trans. Inf. Theory*, vol. 54, no. 12, pp. 5396-5410, Dec. 2008.

[21] *Encyclopedia of Sparse Graph Codes*, [online]. Available: http://www.inference.phy.cam.ac.uk/mackay/codes

[22] *MOSEK Optimization Software*, [online]. Available: http://www.mosek.com